Mass Dependence of Iron Isotope Fractionation in Fe(II)–Fe(III) Electron Exchange Equilibration

Yasuhiko Fujii[a,b], Sang-Ho Kim[a,c], Masao Nomura[a], and Fumiaki Kawakami[a]

[a] Research Laboratory for Nuclear Reactors, Tokyo Institute of Technology, O-okayama, Meguroku, Tokyo 152-8550, Japan

[b] Present address: ATOX Co., Ltd. Takada, Kashiwa. Chiba 177-0861, Japan

[c] Present address: Nano Convergance Practical Application Center, 891–5, Daecheon-Dong, Dalseo-Gu, Daegu, 704-801, Republic of Korea

Reprint requests to Y. F.; E-mail: fujiiya@mopera.net

Z. Naturforsch. **68a,** 79 – 84 (2013) / DOI: 10.5560/ZNA.2012-0095
Received September 9, 2012 / published online February 15, 2013

Dedicated to Professor Alfred Klemm on the occasion of his 100th birthday.

A one hundred meter long ion-exchange chromatograph was used to establish rigorously the mass effects in the iron isotope fractionation in the Fe(II)–Fe(III) electron exchange equilibration. We used a highly porous, strongly basic anion exchange resin packed in glass columns. The abundance ratios of all natural iron isotopes, ^{54}Fe, ^{56}Fe, ^{57}Fe, and ^{58}Fe, in the effluent at the iron adsorption band boundary were measured with a mass spectrometer. The enrichment correlations among these isotopes were analyzed by three-isotope plots. The results clearly showed that the isotope fractionation of Fe(II)–Fe(III) is governed by the normal mass effect; the iron isotope fractionation is not proportional to the nuclear size, but proportional to the reduced mass difference of the pair of iron isotopes.

Key words: Isotope Fractionation; Iron Isotopes; Isotope Effect; Anion Exchange Resin; Chromatography; Oxidation-Reduction Reaction.

1. Introduction

Mass independent fractionation (MIF) is a very interesting topic of isotope chemistry. In addition to the well-known MIF of light elements such as oxygen and sulfur, MIF due to nuclear volume effects was observed in the chemical isotope effects of heavy elements. A prime example of the experimentally observed nuclear size and shape effects of isotope fractionation was reported on uranium chemical isotope effects in U(IV)-U(VI) electron exchange systems. The uranium isotope fractionation between the uranyl (UO_2^{2+}) chloro-complex in an anion exchange resin and the uranous (U^{4+}) ions in an aqueous solution was studied by using a long redox ion exchange chromatograph [1]. The observed uranium isotope fractionation among ^{232}U, ^{233}U, ^{234}U, ^{235}U, ^{236}U, and ^{238}U showed so called 'odd-even staggering' in parallel with the optical isotope shifts in the atomic emission spectral lines of the uranium isotopes; the mass-independent anomaly was observed on the odd mass number isotopes of ^{233}U and ^{235}U. These experimentally observed phenomena have been theoretically explained by Bigeleisen as the nuclear size-and-shape effect in the chemical isotope fractionations [2], and the isotopic fractionation factors α were reproduced by the computation of the energy states of all electrons in the isotopes [3].

Such nuclear size and shape effects were expected to be seen in the isotope fractionations of the lanthanide elements, the nuclear shapes of which are deformed. The isotope fractionation of gadolinium in ethylene diamine tetraacetic acid (EDTA) complex formation has been studied by using ion exchange chromatography [4]. The isotope fractionation coefficients, $\varepsilon = \alpha - 1$, have been determined for ^{155}Gd, ^{156}Gd, ^{157}Gd, and ^{158}Gd against ^{160}Gd. While the even mass number isotopes ^{156}Gd, ^{158}Gd, and ^{160}Gd have shown the normal mass effect, i. e. ε is proportional to the mass difference, the odd mass number isotopes of ^{155}Gd and ^{157}Gd have shown the mass-independent anomaly; the odd-mass-number isotopes do not follow the relation exhibited by the even number isotopes. The values

of the isotopic fractionation coefficients have shown a very similar pattern with the nuclear charge distribution parameter $\delta\langle r^2\rangle$ of the concerned gadolinium isotopes. The chemical isotope effects of gadolinium are highly affected by the nuclear size and shape. Nishizawa et al. reported nuclear field shift effects in the isotope exchange reaction of chromium(III) [5]. Recently the attention has been directed to the nuclear size effect, or field shift effect, on the isotope fractionation of transition elements [6].

On the other hand, in our previous work on barium isotope fractionation in amalgam electrolysis, a normal mass dependence was observed among the stable isotopes of ^{130}Ba, ^{132}Ba, ^{134}Ba, ^{137}Ba, and ^{138}Ba [7]. Recently, the normal mass dependence of isotope fractionation was also observed in the crown ether adsorption of calcium ions [8]. Naturally occurring iron consists of the stable isotopes of ^{54}Fe, ^{56}Fe, ^{57}Fe, and ^{58}Fe. These isotopes, with three even mass numbers and one odd one, draw our attention to the mass dependence of iron isotope fractionation in Fe(II)–Fe(III) electron exchange equilibration.

Iron isotope fractionation has been intensively studied in the fields of geochemistry and environmental chemistry. Experimental and theoretical studies have been made on the isotope effects of ferric and ferrous ions by Johnson et al. [9], Anbar et al. [10], and Hill and Schauble [11]. Anbar et al. studied the iron(III) isotope fractionation by means of ion-exchange chromatography [12] and observed the isotope fractionation ε for $^{54}\mathrm{Fe}-^{56}\mathrm{Fe}$ to be $1\cdot10^{-4}$ and ε for $^{54}\mathrm{Fe}-^{57}\mathrm{Fe}$ to be $1.5\cdot10^{-4}$. The results show the normal mass dependence. To discriminate the small difference between the normal and the anomalous mass dependence due to nuclear volume effects, it is necessary to expand the observed isotopic deviation in the isotopic abundance ratio by multiple-separation process, such as a chemical isotope separation process. For this purpose, ion-exchange chromatography is the most appropriate technique. The migration of the iron adsorption band over 100 m in an ion-exchange chromatography experiment was therefore used in the present work.

2. Experimental

A long chromatographic migration of 100 m was used to study the precise mass dependence of the iron isotope fractionation in the Fe(II)–Fe(III) electron exchange equilibrium. The chromatographic experiment used five glass columns (0.8 cm I.D., 100 cm long, each) packed uniformly with a highly porous, strong base anion exchange resin supported in silica beads (diameter 60 µm). The experimental apparatus is depicted in Figure 1. Prior to the chromatography, the resin was pretreated with HCl solutions to remove impurities and convert itself into Cl^- form. Then a Fe(III) solution (0.1 M $FeCl_3$ in 4 M HCl) was fed into the columns until the entire resin was converted to Fe(III) chloro-complex form. Thereafter a Ti(III) solution (0.1 M $TiCl_3$ in 4 M HCl) was fed into the column system as a reducing eluent. The flow rate of the eluent was 36 ml/hr, and the velocity of the boundary migration was 7 cm/hr. The eluted column was washed with 4 M HCl solutions and regenerated by feeding the above-mentioned Fe(III) solution to repeatedly use the columns for the long-migration redox chromatography. The chromatographic operation continued for 60 days at 80 °C (353 K), until the total migration distance of the adsorption band boundary reached 100 m. Then the effluent samples in the band boundary region were subjected to chemical and isotope analysis.

The ion concentration of each sample fraction was measured with an inductively coupled plasma (ICP)

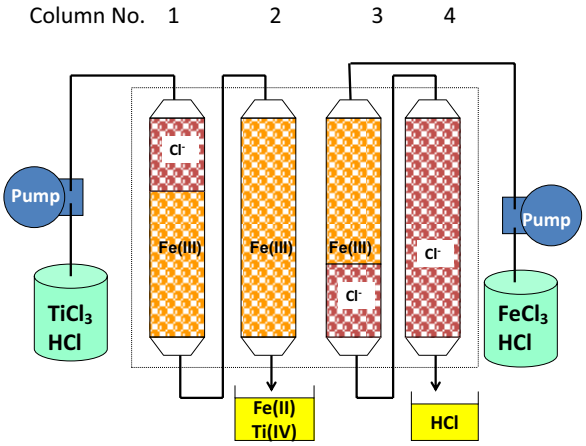

Fig. 1 (colour online). Experimental column system for the 100 m chromatographic migration of the Fe(III) adsorption band. The present figure shows an operational state. A reducing reagent, Ti(III) solution, is fed into Column 1 and the reduced species Fe(II) and oxidized species Ti(IV) are eluted out of Column 2. To regenerate the columns, an Fe(III) solution is fed into Column 3. When the Fe(III) band is eluted out of Column 1, the reducing reagent is fed into Column 2, which is connected to regenerated Column 3. Then the Fe(III) solution for the regeneration is fed to Column 4, connected to Column 5, which is not shown here.

emission spectrometer. Then each effluent fraction was purified for isotope analysis by a small anion exchange column, where iron was adsorbed and separated from titanium. Iron was then eluted with pure water and recharged to a small cation-exchange column. The adsorbed iron in the cation-exchange resin was eluted with 4 M HNO_3. The eluted samples were heated to dryness to decompose organic impurities and re-dissolved with HNO_3.

Then the isotope abundance ratios of the samples were determined with a MAT 261 mass spectrometer equipped with a thermal ionization ion source. The ionization was carried out by means of the double filament method; the time dependence of the measured isotopic ratio is smaller than that found with the single filament method. To measure all isotopic abundance ratios of ^{54}Fe, ^{56}Fe, ^{57}Fe, and ^{58}Fe, care was taken against the mixing of isobars such as ^{54}Cr (2.38% of natural Cr) and ^{58}Ni (67.76% of natural Ni). To eliminate the interference of isobars, other isotopes of chromium and nickel, such as ^{53}Cr and ^{60}Ni, were monitored, and the calculated quantities of ^{54}Cr and ^{58}Ni, on the assumption of the natural abundance, were subtracted from the corresponding iron isotope mass peaks.

3. Results and Discussion

A very sharp boundary was created at the rear of the Fe(III) adsorption zone. During the elution, the isotopic exchange reaction takes place between the iron ions in the solution and in the ion exchange resin. The exchange reaction is expressed for the isotopic pair ^{54}Fe and ^{56}Fe as follows:

$$^{56}\mathrm{Fe(II)} + \underline{^{54}\mathrm{Fe(III)}} = {}^{54}\mathrm{Fe(II)} + \underline{^{56}\mathrm{Fe(III)}}, \quad (1)$$

where the underline represents the species adsorbed in the resin phase. When one of the isotopes is preferentially enriched in one phase, the isotopic equilibrium constant of the above exchange reaction deviates from unity. The isotope fractionation factor α, which is frequently referred to as the separation factor, is defined for the isotopic pair i and j as

$$^{i/j}\alpha = 1 + {}^{i/j}\varepsilon = \left[{}^{i}\mathrm{Fe(II)}\right]\left[\underline{{}^{j}\mathrm{Fe(III)}}\right] \Big/ \left[{}^{j}\mathrm{Fe(II)}\right]\left[\underline{{}^{i}\mathrm{Fe(III)}}\right]. \quad (2)$$

The concentration profile of the iron ions in the effluent and the observed isotopic ratios of ^{54}Fe/^{56}Fe, ^{57}Fe/^{56}Fe, and ^{58}Fe/^{56}Fe in the sample fractions are presented in Figure 2. It is seen that the heavier isotopes are enriched in the rear boundary region, which means that the above exchange reaction, Reaction (1), slightly favours the right-hand side and the heavy isotope is enriched in Fe(III). The tendency of an heavy isotope enrichment in Fe(III) is in accordance with the results obtained by Anbar et al. [10], Welch et al. [13], and Kim et al. [14]. The values of ε, referred to as the isotopic fractionation coefficient, are calculated from the experimentally obtained concentration profiles of iron and the isotopic abundance ratios. The calculation procedure for ε has been dis-

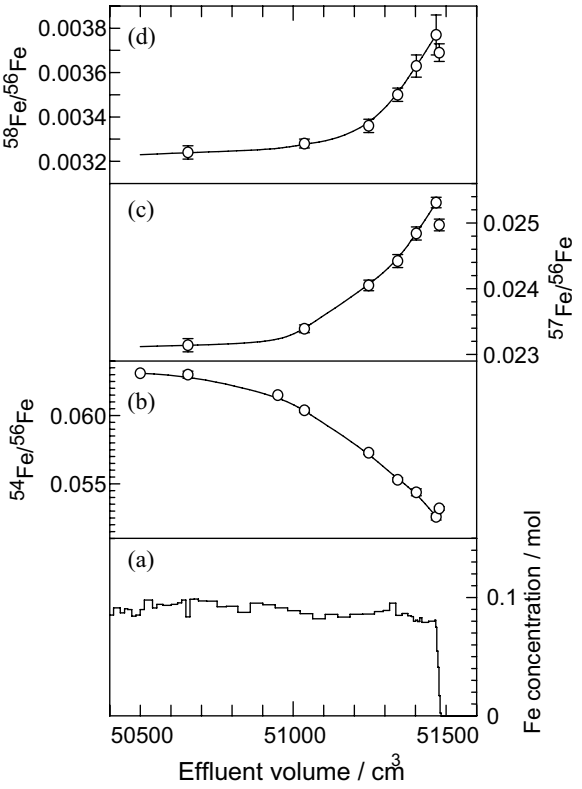

Fig. 2. Iron isotope enrichment at the rear band boundary of the chromatogram after 100 m migration. (a) Concentration of iron in the effluent at the band boundary. (b) Measured isotopic abundance ratios of ^{54}Fe/^{56}Fe in the sampled fractions. Since the heavier isotopes are enriched, ^{54}Fe is depleted against ^{56}Fe at the boundary region. (c) Measured isotopic abundance ratios of ^{57}Fe/^{56}Fe in the sampled fractions. (d) Measured isotopic abundance ratios of ^{58}Fe/^{56}Fe in the sampled fractions.

cussed in previous papers [1, 4, 14]. The calculated values of ε are $(7.9 \pm 0.8) \cdot 10^{-4}$, $(3.6 \pm 0.3) \cdot 10^{-4}$, and $(6.4 \pm 1.3) \cdot 10^{-4}$ for the isotopic pairs ^{54}Fe – ^{56}Fe, ^{57}Fe – ^{56}Fe, and ^{58}Fe – ^{56}Fe, respectively. The approximate value of 0.8‰ at 80 °C for the fractionation of ^{54}Fe – ^{56}Fe is much larger than the value of ε, $1 \cdot 10^{-4}$ experimentally observed by Anbar [12] on the ligand-exchange system of the Fe(III)aq–Fe(III)$_{\text{chloro-complex}}$ by using anion exchange chromatography. However, the presently observed value of 0.8‰ is much smaller than the experimentally obtained values of 2.76‰ at 22 °C by Welch et al. [13], and 2.75‰ at 22 °C by Johnson et al. [9] for the isotope fractionation between Fe(II)–Fe(III). Based on the experimental data, Welch et al. proposed the temperature dependence of the isotope fractionation in Fe(II)–Fe(III) exchange to be

$$1000 \ln \alpha_{\text{Fe(II)–Fe(III)}} = (0.334 \pm 0.032) \cdot 106/T^2 - 0.88 \pm 0.38 . \quad (3)$$

By using this equation, $\ln \alpha_{\text{Fe(II)–Fe(III)}}$ at 80 °C is 1.8‰. This value is still twice as large as the observed fractionation in the present work. The reason for this difference could be the acidity of the present experimental system where 4 M HCl solutions were used as eluent. In the solutions, probably Fe(III) is in the form of tetrahedral $FeCl_4^-$ ions and Fe(II) is in the form of octahedral $FeCl_{1\sim2}(H_2O)_{5\sim4}$.

In the present work, the above-mentioned fractionation coefficients for the different pairs of isotopes were independently determined from the enrichment curves shown in Figure 1. In order to understand the intricacy of the correlation between the isotope fractionation coefficient and the isotopic mass, a detailed analysis can be made by means of the three-isotope-plot method. The measured abundance ratio ${}^{i/j}r_s = ([{}^i\text{Fe}]/[{}^j\text{Fe}])_s$ of isotopes i and j in a sample number s divided by the original isotopic ratio ${}^{i/j}r_0$ gives the local enrichment factor ${}^{i/j}\beta_s = {}^{i/j}r_s/{}^{i/j}r_0$ of sample s. By taking ^{54}Fe and ^{56}Fe as a reference pair of isotopes, the isotopic enrichment correlation is analyzed. In Figure 3, the measured $\ln[{}^{57/56}\beta_s]$ and $\ln[{}^{58/56}\beta_s]$ of sample fraction s are plotted against $\ln[{}^{56/54}\beta_s]$ of the same sample. Figure 3 is so called 'three-isotope plot'. The slopes of the lines in Figure 3 yield correlation factors for the isotopic pair ^{54}Fe – ^{56}Fe vs. ^{56}Fe – ^{57}Fe as 0.48 ± 0.01 and for the isotopic pair ^{54}Fe/^{56}Fe vs. ^{56}Fe/^{58}Fe as 0.92 ± 0.04.

The slopes observed in the three-isotope plots are listed in Table 1 along with the fractionation coefficients observed in the present work. Table 1 also lists

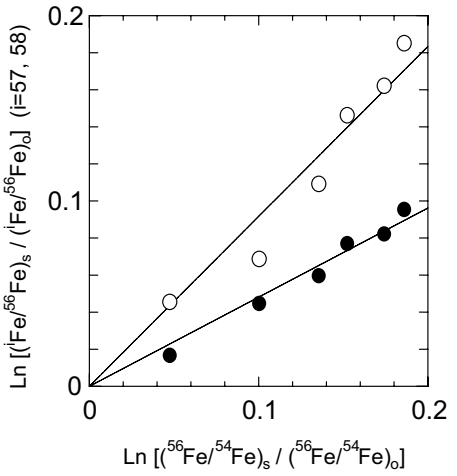

Fig. 3. Three-isotope plots of measured isotopic abundance ratios. The local enrichment factors, defined as ${}^{i/j}r_s/{}^{i/j}r_0$, where the common isotope $j = {}^{56}$Fe, $i = {}^{57}$Fe (solid circle) or ^{58}Fe (open circle), are plotted against the local enrichment factor of the isotopic pair ^{54}Fe and ^{56}Fe in a logarithmic scale; the subscript s represents the sample number, and o represents the original feed. A correlation between two pairs of isotopes is obtained from the slope of the plots θ_i : $\theta_{i=57} = 0.48 \pm 0.01$ and $\theta_{i=58} = 0.92 \pm 0.04$: the error range of the slope means the standard error.

the isotopic properties of the iron isotopes; the mass difference $(M_j - M_i)$, the reduced mass difference $(M_j - M_i)/M_iM_j$, the nuclear size difference $\delta\langle r^2\rangle$, and the optical isotope shifts in the emission spectral lines. To compare the isotope fractionation with the nuclear properties, relative values of all these terms are calculated and listed in Table 1. Apparently, if we carefully compare the mass dependence of the slopes of the three-isotope plots, it is seen that the chemical isotope effect is not directly related to the nuclear radius difference. The difference in the nuclear radius $\langle r^2\rangle$ between ^{56}Fe and ^{58}Fe is clearly smaller than the deviation between ^{54}Fe and ^{56}Fe; $\delta\langle r^2\rangle$ of the pair ^{56}Fe – ^{58}Fe is 87% of ^{54}Fe and ^{56}Fe [15].

Then the slope of the three-isotope plots is compared with the relative values of the 'reduced mass difference' in Table 1, where the relative values of the pairs ^{56}Fe – ^{57}Fe and ^{56}Fe – ^{58}Fe against the reference pair of ^{54}Fe – ^{56}Fe are shown to be 0.475 and 0.932, respectively. The experimentally observed slopes of 0.48 ± 0.01 for the pair ^{56}Fe – ^{57}Fe and of 0.92 ± 0.04 for the pair ^{56}Fe – ^{58}Fe are in good agreement with the above-mentioned relative values of the reduced mass differences.

Table 1. Nuclear mass and size of iron isotopes and experimentally observed isotope effects.

Isotopic property	Isotopic pair ^{54}Fe–^{56}Fe	^{57}Fe–^{56}Fe	^{58}Fe–^{56}Fe
Mass difference (amu)	1.9953	1.0004	1.9983
Relative value	1	0.501	1.0015
Reduced mass difference $\times 10^4$ (amu^{-1})	6.61	3.14	6.16
Relative value	1	0.475	0.932
Nuclear size $\delta\langle r^2\rangle$ (fm^2)	0.327 ± 0.008	0.12	0.286 ± 0.007
Relative value	1	0.37	0.87
Optical isotope shift (MHz)	1684.5 ± 1.6	842.4 ± 1.6	1602.0 ± 1.6
Relative value	1	0.500	0.951
Separation coefficient $\varepsilon \times 10^4$	7.9 ± 0.8	3.6 ± 0.3	6.4 ± 1.3
Relative value	1	0.46 ± 0.04	0.81 ± 0.16
Slope of three-isotope plot	1	0.48 ± 0.01	0.92 ± 0.04

The relative values are calculated, by taking the isotopic pair ^{54}Fe–^{56}Fe as a reference. The unit 'amu' is the atomic mass unit; ^{54}Fe = 53.9396, ^{56}Fe = 55.9349, ^{57}Fe = 56.9353, and ^{58}Fe = 57.9332. The optical isotope shifts are reported values of the emission spectral line 305.908 nm [16].

The classical theory of the chemical isotope effects in equilibrium explains that the origin of these effects, or isotope fractionation, is a quantum effects in the vibration of isotopic molecules. In the cases where an isotopic pair i and j is concerned, the isotopic fractionation is proportional to the mass difference $(M_j - M_i)$, as a first approximation, and more precisely to the reduced mass difference, $(M_j - M_i)/M_iM_j$. It is thus a reasonable conclusion that the chemical isotope fractionation of the iron isotopes shows a normal mass dependence, since iron is a light element with a small nucleus compared with the actinide and the lanthanide elements, which show anomalous isotope effects due to the nuclear volume effects.

However, the 'normal mass dependence' does not necessarily mean that the origin of the chemical isotope effects of the Fe(II)/Fe(III) system is a molecular vibration of these species. A similarity is seen between the slopes of the three-isotope-plot and the optical isotope shifts. The reported optical isotope shifts of iron at the emission line 305.908 nm are presented for the concerned isotopic pairs in Table 1 in units of MHz [16]. If we compare the relative values of these isotopic properties, it is seen that both the optical isotope shifts and the three-isotope-plot slopes show a very similar pattern of mass dependence. Probably both isotope effects, the chemical isotope fractionations and the optical isotope shifts, are mainly due to the nuclear mass effects rather than to the nuclear size effects. Since the optical isotope shifts show the isotopic differences in the electronic states, the influences of the electronic state may not be completely excluded in understanding the phenomena of the isotope fractionation in Fe(II)/Fe(III) exchange system, although the isotope fractionation in Fe(II)–Fe(III) exchange has been theoretically explained by the molecular vibration [11]. Optical isotope shifts, reported for many elements [15], are useful for understanding the phenomena of chemical isotope fractionation.

4. Conclusions

Long distance redox chromatography was performed to study the mass dependence of the iron isotope fractionation in an Fe(II)–Fe(III) exchange reaction by using anion exchange columns. A precise analysis of the isotopic abundance ratios of iron samples in the effluent of the chromatogram allows to clarify the isotope fractionation and to demonstrate a normal mass dependence, where the fractionation coefficients are proportional to the reduced mass difference. Similarly, this is seen in the mass dependences of both isotope effects in the Fe(II)–Fe(III) chemical exchange reaction and in the isotope shifts of the iron isotopes in their atomic emission spectral lines. The three-isotope-plot is a useful technique to observe the precise mass dependence of chemical isotope fractionation rather than the separation coefficient determined independently for each isotopic pair.

Acknowledgements

We thank Prof. Takanobu Ishida for his valuable comments. The present work was partly supported by a Grant-in-Aid for Science Research Program of the Ministry of Education, Science, Technology, Sports and Culture, Japan.

[1] M. Nomura, N. Higuchi, and Y. Fujii, J. Am. Chem. Soc. **118**, 9127 (1996).
[2] J. Bigeleisen, J. Am. Chem. Soc. **118**, 3676 (1996).
[3] M. Abe, T. Suzuki, Y. Fujii, M. Hada, and K. Hirao, J. Chem. Phys. **133**, 44309 (2010).
[4] I. M. Ismail, A. Fukami, M. Nomura, and Y. Fujii, Anal. Chem. **72**, 2841 (2000).
[5] T. Fujii, D. Suzuki, K. Gunji, K. Watanabe, H. Moriyama, and K. Nishizawa, J. Phys. Chem. A **10**, 6911 (2002).
[6] T. Fujii, F. Moynier, P. Telouk, and M. Abe, J. Phys. Chem. A **114**, 2543 (2010).
[7] C. Zheng, M. Nomura, K. Motomiya, and Y. Fujii, J. Chem. Soc., Faraday Trans. **92**, 4485 (1996).
[8] Y. Fujii, M. Nomura, T. Kaneshiki, Y. Sakuma, T. Suzuki, S. Umehara, and T. Kishimoto, Isotop. Environ. Health Stud. **46**, 233 (2010).
[9] C. R. Johnson, J. L. Skulan, B. L. Beard, H. Sun, K. H. Nelson, and P. S. Braterman, Earth Planet. Sci. Lett. **195**, 141 (2002).
[10] A. D. Anbar, A. A. Jarzecki, and T. G. Spiro. Geochimi. Cosmochimi. Acta. **69**, 825 (2005).
[11] P. S. Hill and E. A. Schauble, Geochimi. Cosmochimi. Acta. **72**, 1939 (2008).
[12] A. D. Anbar, J. E. Roe, J. Barling, and K. H. Nealson, Science **288**, 126 (2000).
[13] S. A. Welch, B. L. Beard, C. M. Johnson, and P. S. Braterman, Geochimi. Cosmochimi. Acta. **67**, 4231 (2003).
[14] S.-H. Kim, M. Aida, M. Nomura, M. R. Nur, and Y. Fujii, J. Ion Exchange **11**, 26 (2000).
[15] W. H. King, Isotope Effects in Atomic Spectra, Plenum Publishing Corp., New York 1984.
[16] D. M. Benton, E. C. A. Cochrane, and J. A. R. Griffith, J. Phys. B: At. Mol. Opt. Phys. **30**, 5359 (1997).